Development of biochars from pyrolysis of lotus stalks for Ni(II) sorption: using zinc borate as flame retardant

Hai Liu[a], Shuang Liang[a,*], Jinhong Gao[a], Huu Hao Ngo[b], Wenshan Guo[b], Zizhang Gou[a], Yiran Li[a]

[a]*Shandong Key Laboratory of Water Pollution Control and Resource Reuse, School of Environmental Science and Engineering, Shandong University, Jinan 250100, China*

[b]*School of Civil and Environmental Engineering, University of Technology Sydney, Broadway, NSW 2007, Australia*

Abstract

In this work, zinc borate (ZB) was employed as flame retardant for preparation of biochar (BC). A series of BC samples were generated by varying the ZB to lotus stalks (LS) ratio (0.25, 0.5 and 1.0) under different temperatures (300, 350 and 400 °C) for 1 h. The BCs were analyzed for their surface morphologies, surface areas, surface elemental compositions and yields. The results indicated that, after charring, ZB kept the structures of the produced BCs as its starting material (LS), dramatically enhancing their yields, and promoting their surface oxygen content. The BCs were used as adsorbent for removal of Ni(II) from aqueous solutions. Sorption of Ni(II) on the BCs was enhanced about 3-10 times compared with that of BCs derived from pyrolysis of LS without adding ZB.

Keywords: Zinc borate; Biochar; Ni(II)

Corresponding author.
Tel.: +86 531 88361712; fax: +86 531 88364513.
E-mail addresses: sliang@live.com, liangshuang@sdu.edu.cn(S.Liang)

1. Introduction

Sorption onto activated carbon has been proven to be a very simple and effective technology for eliminating undesirable heavy metal ions from wastewater. Activated carbon is usually fabricated at high temperatures (≥450 °C) under well-controlled activating conditions. In order to produce activated carbon with a well-developed structure and high yield, the precursor after impregnating with activating agent is activated at high temperatures (≥450 ^{o}C for H_3PO_4 and $ZnCl_2$ activation and ≥700 ^{o}C for KOH and NaOH activation) under inert gas atmosphere (nitrogen). Nevertheless, its high cost precludes its large-scale application in developing countries. However, as another carbonaceous material, biochar (BC) was produced by pyrolysis of biomass under conditions of lower temperatures (≤ 400 ^{o}C) and easier preparation conditions [1-3]. Thus, it shows much lower cost than activated carbon.

Recently, BC has been successfully applied as an effective adsorbent for removal of metal ions from aqueous solution [4-6]. The properties of BC are mainly influenced by its precursors and pyrolysis conditions. The time-temperature pyrolysis profile for various biomasses was discussed thoroughly in previous publications [7-9]. However, little information is available on addition of flame retardant for BC production.

During the past decade a very large number of zinc borate (ZB) was employed as a highly efficient flame retardant for polymer materials [10-13]. ZB contains both zinc oxide and boric oxide and acts as multifunctional flame retardant. During thermal treatment, ZB functions not only as fire retardant, but as highly effective smoke suppressant and corrosion inhibitor [14].

The objectives of this paper are 1) to study the effect of additive amount of ZB and charring temperature (300, 350 and 400 ^{o}C) on the textural and chemical properties of produced BCs; and 2) to evaluate the sorption capacities of produced BCs toward Ni(II) by comparing with the BCs derived from pyrolysis of LS without adding ZB.

2. Materials and methods

2.1. Materials

All the chemical reagents were of analytical grade and were used as purchased. Lotus (*Nelumbo nucifera*), a kind of hydrophytes, has been widely planted as an important and popular cash crop in many Asian countries. Lotus stalks (LS), with porous caudex system and large cell gap, can be used as a low-cost and efficient precursor for BC production. LS were obtained from a wetland located in Shandong, China. After harvest, the LS were washed several times with distilled water, dried at 105 °C for 24 h and crushed to pieces of approx. 0.45-1.0 mm. ZB ($2ZnO{\cdot}3B_2O_3{\cdot}3.5H_2O$) with particle size of 1~2 μm was used as flame retardant. Ni^{2+} solution was prepared by dissolving a weighed quantity of analytical grade $Ni(NO_3)_2{\cdot}6H_2O$ in distilled water.

2.2. Preparation of BCs

About 10 g of LS were fully mixed with a weighted amount of ZB and 20 mL

distilled water, and the mixed samples were then dried at 105 ^{o}C for 9 h to remove moisture. The ratio (*R*, g ZB/g LS) was chosen from 0.25:1.0 to 1.0:1.0. After drying, the samples were then placed in 150 mL ceramic crucibles, and each ceramic crucible was covered with a fitting lid. The samples were charred at 300, 350 and 400 °C for 1 h under oxygen-limited conditions in a muffle furnace (combustion chamber, 300 * 200 * 120 mm). In order to evaluate the effect of ZB addition on the yields and physicochemical properties of the final BCs, another three BC samples were also prepared from LS without adding ZB at charring temperature of 300, 350 and 400 ^{o}C for 1 h. After cooling to room temperature, the resulting charred residues were pulverized for subsequent demineralization with 0.5 mol/L HCl. Then, the samples were thoroughly washed with distilled water until the washing liquids attained a constant pH, filtered and dried for 9 h at 105 °C. The BC samples were hereafter referred to as BC-X-Y, with X and Y indicating the final charring temperature (300, 350 and 400 °C) and the *R* (0, 0.25, 0.5, and1.0), respectively.

2.3. Characterization methods

The thermo-gravimetric analysis (TGA) and derivative thermogravimetric (DTG) curves of the raw LS and the mixture of LS and ZB were obtained by using a thermo-gravimetric analysis (TGA-50 analyzer). The samples were referred to as LS-X-Y, with X and Y indicating the final charring temperature (300, 350 and 400 °C) and the ratio (g ZB/g LS; 0, 0.25, 0.5, and1.0), respectively. Each sample was heated up to a designed temperature and kept at this temperature for 1 h at a heating rate of

10 °C/min.

The BET surface area (S_{BET}) of BCs was determined by adsorption of N_2 at 77 K using a surface area analyzer (Quantachrome Corporation, USA). The S_{BET} was calculated from the isotherms using the Brunauer-Emmett-Teller (BET) equation. The surface texture of the BCs was observed by using a scanning electron microscope (SEM Hitachi S4800, Japan). The surface elemental composition of BCs was determined using energy-dispersive spectrometer (EDS).

2.4. Nickel sorption

Sorption experiments were carried out with the initial concentration of Ni^{2+} in the range of 20-80 mg/L. The sorption dose was 600 mg/L using 100 mL flask. The initial pH was adjusted with addition of 0.01 M HCl or NaOH to the value of 6.00 ± 0.02. The flasks were kept in an isothermal water bath and agitated at 120 rpm for 48 h to ensure that equilibrium was reached. The amount of Ni(II) adsorbed at equilibrium (Q_e, mg/g) was calculated by the equation: $Q_e = (C_0\text{-}C_e)V/W$, where C_0 and C_e are the initial and equilibrium concentration of Ni(II) (mg/L); V represents the solution volume (L); and W is the mass of adsorbent (g).

3. Results and discussion

3.1. Thermo-gravimetric analysis of LS-X-Y samples

The TGA and DTG curves obtained from the thermo-gravimetric analysis of LS-X-Y samples are shown in Fig. 1. The weight loss for the samples during

thermo-gravimetric analysis could be divided in to three stages. In the first stage, the small amount of weigh loss as temperature ranged from room temperature to 200 ^{o}C was due to the loss of water and light volatile compounds in LS. A significant weight loss occurred in the second stage, as temperature increased from 200 ^{o}C to the final temperature (300, 350 or 400 ^{o}C), which was mainly attributed to the evolution of volatile compounds generated by decomposition of hemicellulose, cellulose and lignin in LS. In the third stage, as temperature kept at a constant value of 300, 350 or 400 ^{o}C, the samples displayed a continuous and slight weight loss.

It can be seen from Fig.1a that LS-X-Y (Y>0) samples displayed much lower weight loss than LS-X-0 samples and their weight losses started at higher temperature than LS-X-0 samples. These results indicated that ZB has good flame-retardant performance for LS. The DTG curves of the samples heating at same conditions showed a maximum peak at the same temperatures. Compared with LS-350-Y and LS-400-Y samples, LS-300-Y samples exhibited more obvious a weight loss for the third stage, indicating the incomplete charring of LS-300-Y samples. ZB started decompose at about 290 ^{o}C by liberating water, boric acid and boron oxide. The boric acid and soften boron oxide at temperature > 350 ^{o}C could promote the dehydration and formation of a carbonized layer [11]. Thus, for LS-300-Y samples (Y>0), LS-300-0 showed the highest maximum decomposition rate, while, for LS-350-Y and LS-400-Y samples(Y>0), LS-350-0 and LS-400-0 samples exhibited lower maximum decomposition rates than the other LS-350-Y and LS-400-Y samples.

3.2. Physical and chemical characteristics and yield of BC

SEM images of the BCs are shown in Fig. 2. After charring, BC-300-Y samples showed a similar structure to LS, while the structures of BC-350-Y and BC-400-Y samples were obviously corroded. Compared with the other BC-X-Y samples, the structures of BC-X-0 samples were more severely corroded. Some particles or flakes on the surfaces of BC-X-0 samples were observed, which could be attributed to the chemical vapor deposition of pyrolysis products. The surfaces of BC-X-Y samples (Y>0) were more smooth than BC-X-0 samples resulting from the formation of carbonization layer promoted by the presence of ZB and its good afterglow suppressant performance.

As shown in Table 1, the BET surface area of BC-X-0 samples increased with increasing pyrolysis temperature. The production of volatile compounds inside the LS particles gradually increased with increasing final temperature, resulting in increase of porosity [15]. The BC-X-Y samples (Y **>** 0) got the highest surface areas at temperature of 300 ^{o}C. This result may be due to the formation for boric acid decomposed by ZB that made the BCs' surfaces smooth at high temperature.

For the external heating (muffle furnace), thermal energy is supplied to the surface of sample and then transferred inside by heat conduction, and therefore it is difficult to achieve a uniform temperature for the sample [16]. As a result, the internal and external elemental composition of the produced BC would be different [17]. Surface elemental compositions of the BCs are shown in Table 1. The relatively higher values of O/C for BC-X-Y samples (Y **>** 0) compared with BC-X-0 samples indicated that

more O-containing groups existed on their surfaces. As the most active minor element in biochar, the oxygen atoms can be present in various forms of surface functional groups. At high temperature ZB could form an impervious layer on the surface of LS, promote the formation of char at the surface of LS and prevent the release of combustible gases from the surface of LS. These properties of ZB promoted the carbonation lignocellulosic materials and also preserved its surface oxygen content. Zinc and boron were not detected in these samples, indicating Zn and B compounds were removed in the washing stage.

The yields of each BC were recorded in Table 1. The yield is defined as the % ratio of weight of BC produced to the weight of LS utilized for charring. Yields of the BCs declined with increasing temperature and increased with increasing the amount of ZB added. The yields of BC-X-Y samples (Y > 0) were dramatically much higher than BC-X-0 samples.

3.3. Ni(II) sorption capacities of BC

The sorption isotherms of Ni(II) onto the BCs were studied at different initial Ni(II) concentrations ranging from 20 to 80 mg/L and are shown in Fig. 3. In order to estimate the maximum sorption capacity and the sorption intensity of Ni(II) onto the BCs, Langmuir ($Q_e = Q_m K_L C_e/(1 + K_L C_e)$) and Freundlich ($Q_e = K_F C_e^{1/n}$) isotherm models are conducted to simulate the sorption. Herein, Q_e (mg/g) is the amount adsorbed; C_e (mg/L) is the equilibrium concentration; Q_m (mg/g) is the maximum sorption capacity; K_L is the Langmuir sorption constant; and K_F and 1/n are the

Freundlich constants.

The constants of Langmuir and Freundlich models fitting into the sorption data were listed in Table 2. The values of correlation coefficient (R^2) obtained from Langmuir model were much higher than those obtained from Freundlich model, which indicated that the sorption of Ni(II) on the BCs was simulated better by Langmuir model than by Freundlich model. It can also be observed from Fig. 3 that the Langmuir model fits the data better. The *1/n* values of the BCs were between 0 and 1, representing a favorable sorption of Ni(II) onto the BCs.

As shown in Table 2 and Fig 3, the sorption capacity of Ni(II) onto the BC-X-Y samples obtained its maximum at Y = 0.5 (BC-300-0.5, BC-350-0.5 and BC-400-0.5) for different charring temperatures and at X =300 ^{o}C for different *R* (g ZB/g LS). The considerable Ni(II) sorption capacity of BC-300-Y samples (Y **>** 0) could be attributed to the roles of the higher O-containing groups and non-carbonized biomass fractions in heavy metal immobilization, as proposed by Uchimiya [18]. It is obvious that the Q_m (mg/g) for the BC-X-Y samples (Y **>** 0) was about 3-10 times higher than that on BC-X-0 samples. The higher sorption capacity for Ni(II) may be attributed to their much higher O-containing groups, resulting in more positive sites for Ni(II) sorption by cation exchange, electrostatic attraction or surface complexation.

4. Conclusion

This study investigated the preparation of BCs by using ZB as flame retardant. The obtained promising results indicated that, by comparing to the BC-X-0 samples, 1)

ZB prevented the structure of the BCs from corrosion at high temperature; 2) much more oxygen-containing groups and yields of the BCs were developed by using ZB as flam retardant; 3) using ZB as flame retardant for BC production can dramatically enhanced the Ni(II) sorption capacities of the produced BCs.

Acknowledgements

This work was supported by the Independent Innovation Foundation of Shandong University (2012JC029), Natural Science Foundation for Distinguished Young Scholars of Shandong Province (JQ201216) and National Water Special Project (2012ZX07203-004).

References

[1] Z. Liu, F.-S. Zhang, Removal of lead from water using biochars prepared from hydrothermal liquefaction of biomass, J. Hazard. Mater. 167 (2009) 933-939.

[2] W. Ding, W. Peng, X. Zeng, X. Tian, Effects of phosphorus concentration on Cr(VI) sorption onto phosphorus-rich sludge biochar, Front. Environ. Sci. Eng., (2013) 1-7.

[3] J. Ni, J.J. Pignatello, B. Xing, Adsorption of Aromatic Carboxylate Ions to Black Carbon (Biochar) Is Accompanied by Proton Exchange with Water, Environ. Sci. Technol. 45 (2011) 9240-9248.

[4] T.-Y. Jiang, J. Jiang, R.-K. Xu, Z. Li, Adsorption of Pb(II) on variable charge soils amended with rice-straw derived biochar, Chemosphere 89 (2012) 249-256.

[5] Y. Qiu, Z. Zheng, Z. Zhou, G.D. Sheng, Effectiveness and mechanisms of dye adsorption on a straw-based biochar, Bioresource Technol. 100 (2009) 5348-5351.

[6] L. Beesley, M. Marmiroli, The immobilisation and retention of soluble arsenic, cadmium and zinc by biochar, Environ. Pollut. 159 (2011) 474-480.

[7] Y. Chun, G. Sheng, C.T. Chiou, B. Xing, Compositions and Sorptive Properties of Crop Residue-Derived Chars, Environ. Sci. Technol. 38 (2004) 4649-4655.

[8] B. Chen, D. Zhou, L. Zhu, Transitional Adsorption and Partition of Nonpolar and Polar Aromatic Contaminants by Biochars of Pine Needles with Different Pyrolytic Temperatures, Environ. Sci. Technol. 42 (2008) 5137-5143.

[9] D. Mohan, C.U. Pittman Jr, M. Bricka, F. Smith, B. Yancey, J. Mohammad, P.H. Steele, M.F. Alexandre-Franco, V. Gómez-Serrano, H. Gong, Sorption of arsenic,

237 cadmium, and lead by chars produced from fast pyrolysis of wood and bark during
238 bio-oil production, J. Colloid Interf. Sci. 310 (2007) 57-73.
239 [10] B. Garba, Effect of zinc borate as flame retardant formulation on some tropical
240 woods, Polym. Degrad. Stabil. 64 (1999) 517-522.
241 [11] F. Laoutid, L. Bonnaud, M. Alexandre, J.M. Lopez-Cuesta, P. Dubois, New
242 prospects in flame retardant polymer materials: From fundamentals to
243 nanocomposites, Mat. Sci. Eng. R. 63 (2009) 100-125.
244 [12] H. Pi, S. Guo, Y. Ning, Mechanochemical improvement of the flame-retardant
245 and mechanical properties of zinc borate and zinc borate–aluminum trihydrate-filled
246 poly(vinyl chloride), J. Appl. Polym. Sci. 89 (2003) 753-762.
247 [13] A. Genovese, R.A. Shanks, Structural and thermal interpretation of the synergy
248 and interactions between the fire retardants magnesium hydroxide and zinc borate,
249 Polym. Degrad. Stabil. 92 (2007) 2-13.
250 [14] S. Kim, Flame retardancy and smoke suppression of magnesium hydroxide filled
251 polyethylene, J. Polym. Sci. Pol. Phys. 41 (2003) 936-944.
252 [15] M. Ertaş, M. Hakkı Alma, Pyrolysis of laurel (Laurus nobilis L.) extraction
253 residues in a fixed-bed reactor: Characterization of bio-oil and bio-char, J. Anal. Appl.
254 Pyrol. 88 (2010) 22-29.
255 [16] L.M. Norman, C.Y. Cha, production of activated carbon from coal chars using
256 microwave energy, Chem. Eng. Commun. 140 (1995) 87-110.
257 [17] R. Pietrzak, XPS study and physico-chemical properties of nitrogen-enriched
258 microporous activated carbon from high volatile bituminous coal, Fuel 88 (2009)

1871-1877.

[18] M. Uchimiya, I.M. Lima, K. Thomas Klasson, S. Chang, L.H. Wartelle, J.E. Rodgers, Immobilization of Heavy Metal Ions (CuII, CdII, NiII, and PbII) by Broiler Litter-Derived Biochars in Water and Soil, J. Agr. Food Chem. 58 (2010) 5538-5544.

Figure captions

Fig. 1. TGA and DTG curves of LS-X-Y samples.

Fig. 2. SEM images of the BCs.

Fig. 3. Sorption isotherms of Ni(II) on the BCs.

Table 1 Surface area, surface elemental composition and yields of the BCs.

Samples	S_{BET} (m^2/g)	C (%)	O (%)	O/C (%)	Si (%)	Yield (%)
BC-300-0	9	60.15	39.62	65.87	0.23	38.4
BC-300-0.25	24	48.23	51.63	107.1	0.14	43.1
BC-300-0.5	41	47.49	52.35	110.2	0.16	45.7
BC-300-1.0	45	51.39	48.22	93.83	0.39	50.2
BC-350-0	21	65.83	34.06	51.74	0.11	31.0
BC-350-0.25	24	53.77	46.15	85.83	0.08	36.4
BC-350-0.5	18	52.09	47.86	91.88	0.05	37.9
BC-350-1.0	17	55.78	44.05	78.97	0.17	43.5
BC-400-0	41	72.30	27.47	37.99	0.23	26.9
BC-400-0.25	17	60.79	39.02	64.19	0.19	32.6
BC-400-0.5	26	57.63	41.98	72.84	0.39	34.6
BC-400-1.0	21	62.70	37.17	59.28	0.13	38.6

285 **Table 2** Langmuir and Freundlich constants related to the sorption isotherms of Ni(II) for the BCs.

Samples	Langmuir			Freundlich		
	q_m mg·g^{-1}	k_L L·mg^{-1}	R^2	$1/n$	k_F mg^{1-n}L^n/g	R^2
BC-300-0	6.4	0.456	0.9999	0.059	4.85	0.9761
BC-300-0.25	59.9	0.255	0.9942	0.234	23.5	0.9821
BC-300-0.5	61.7	0.267	0.9987	0.233	24.3	0.9871
BC-300-1.0	49.5	0.288	0.9991	0.194	22.4	0.9689
BC-350-0	10.3	0.226	0.9996	0.109	6.10	0.9988
BC-350-0.25	38.8	0.411	0.9998	0.131	22.5	0.9623
BC-350-0.5	40.8	0.298	0.9996	0.161	20.7	0.9823
BC-350-1.0	38.0	0.266	0.9995	0.166	2.93	0.9603
BC-400-0	10.5	0.321	0.9996	0.078	7.21	0.9977
BC-400-0.25	34.7	0.464	0.9996	0.110	21.8	0.9434
BC-400-0.5	40.0	0.315	0.9988	0.147	21.3	0.9902
BC-400-1.0	29.9	0.348	0.9994	0.119	17.7	0.9452

286

287

288

289

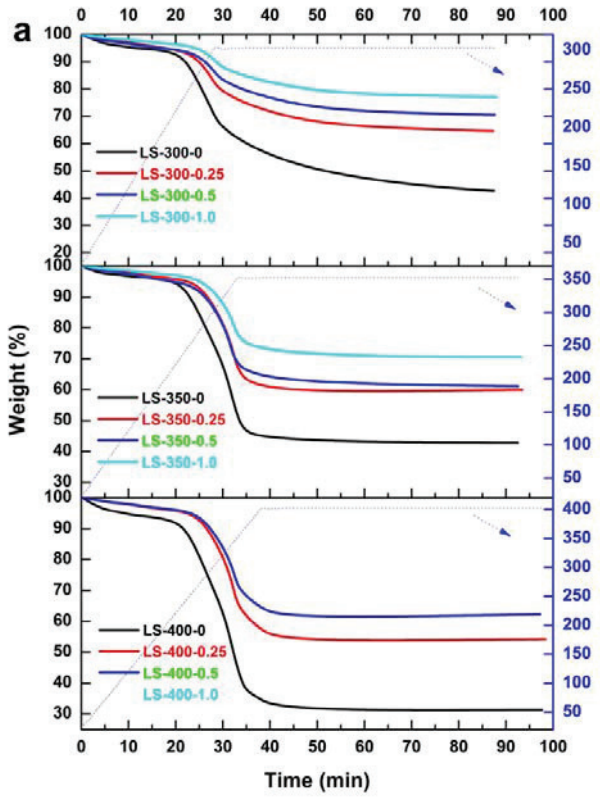

289

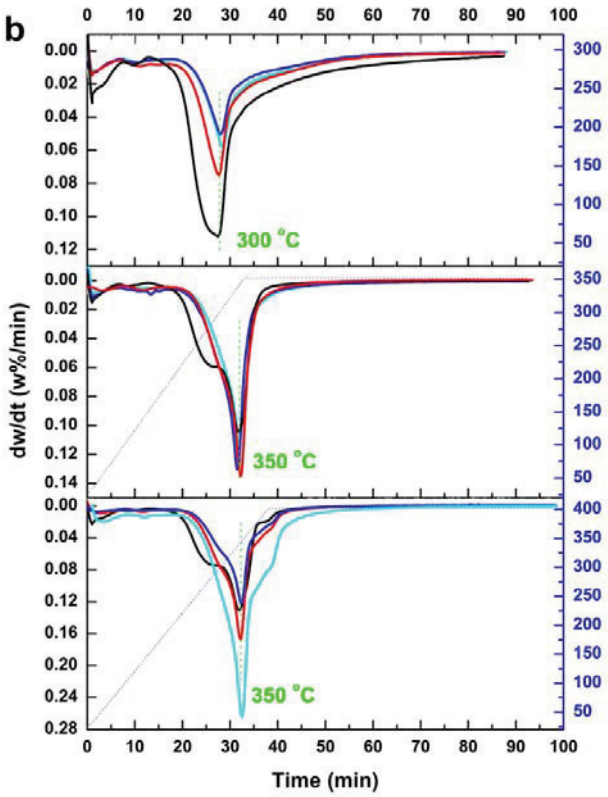

290

291 Fig. 1. TGA and DTG curves of LS-X-Y samples.

292

293

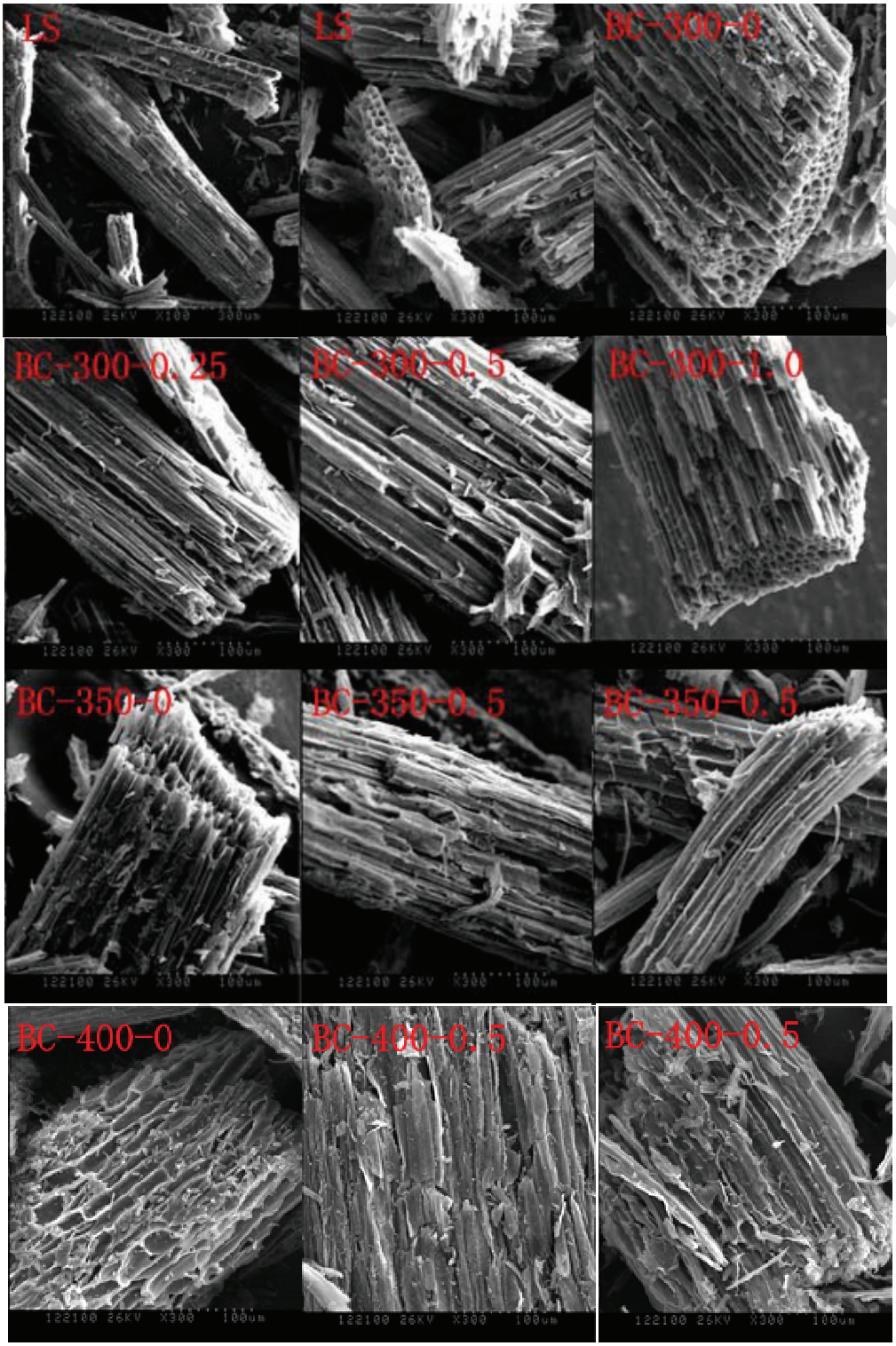

Fig. 2. SEM images of the BCs.

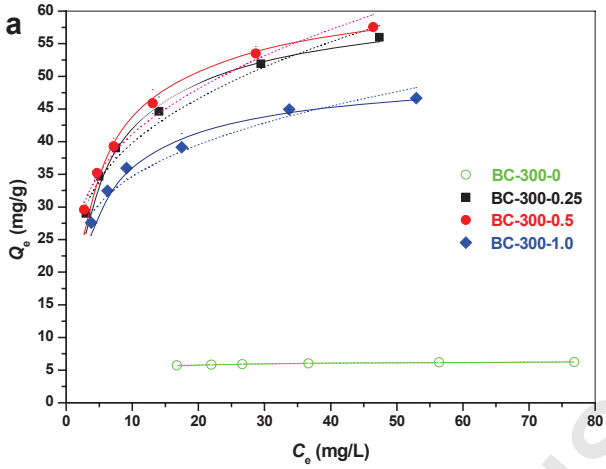

296

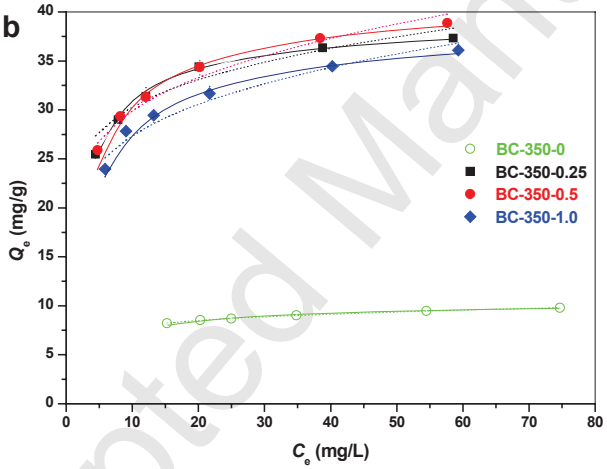

297

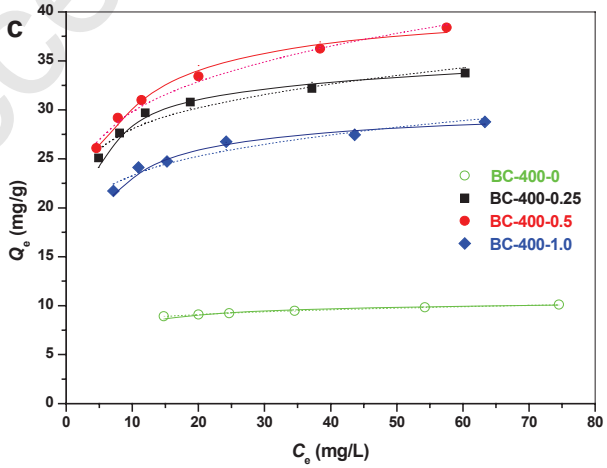

298

299 **Fig. 3.** Sorption isotherms of Ni(II) on the BCs (dosage = 60 mg/100 mL; time = 48 h;

300 and temperature = 22±1 ^{o}C). Solid and dashed lines represent Langmuir model and

301 Freundlich model fitting to the data, respectively.

302